Application of Composite Buildup Factors in Point-Kernel Method for Laminated Gamma Shields

Mario Matijević, Antonia Mesić, Krešimir Trontl, Dubravko Pevec
University of Zagreb Faculty of Electrical Engineering and Computing
Unska 3, Zagreb, Croatia
mario.matijevic@fer.hr, antonia.mesic@fer.hr, kresimir.trontl@fer.hr, dubravko.pevec@fer.hr

ABSTRACT

In practical applications many shields against gamma radiation are often laminated (or composite), using layers of different materials. Such composite shields introduce difficulties for calculating buildup factors, since change in angular and energy distribution of gamma-rays occur during the passage through intervening layers. Additional complication comes from interchangeable materials, since gamma-rays in every layer depend on previous layers, so this memory effect has an implication on layer ordering inside the shield. The accumulated empirical data over history has served as a rich database for introducing several approximations to composite buildup factors, such as methods of Goldstein, Blizard, Broder, and Bowman-Trubey. These methods proved quite useful for applications in gamma-ray shielding when using the deterministic point-kernel (PK) methods. This paper presents underlying analytical derivations and implementation of such methods in our existing PK program for gamma shielding, which is still in a development phase. The selected test-cases were focused on calculating the buildup flux on a point detector, originating from a slab gamma source shielded by a slab shield. The volumetric source has an explicit photon self-absorption, with a constant or exponential gamma-ray emission rate, while both slabs can have variable thickness and shielding materials. The obtained sensitivity study of PK deterministic results was verified using the stochastic Monte Carlo method, to compare similarities and differences in gamma flux components (uncollided and collided) and composite buildup factors.

Keywords: *buildup factor, point-kernel, composite shield, gamma radiation, Monte Carlo method*

1 INTRODUCTION

The point-kernel (PK) method applied to gamma radiation shielding has a rich history of many decades, spanning from the era of first digital computers [1][2]. The analytical ray-tracing algorithms were successfully applied to many real-life problems related to radiation shielding, where action of distributed source of radiation can be interpreted as equivalent summation of radiation from many "differential" source elements of length, surface or volume [3]. These source elements represent basic building blocks emitting photons/sec per unit of length, area or volume. However, inherent limitations of such straightforward approach were noticed early on, especially for describing gamma ray scattering. The absence of refined physical model resulted in non-conservative results, often too low compared to newer computational approaches. For that reason, the concept of tabulated corrective buildup factor (*B*-factor) was introduced by H. Goldstein, to include gamma-ray buildup inside the shields [2]. Over the time, the necessity of *B*-factors inclusion in PK numerical integration led to various analytical expressions [4], such as Taylor, Berger, Capo,

Harima, etc. The right way to use these formulae (according to A. Chilton [5]), derived for point gamma source, is in form of the kernel function when integrating expression for differential flux on the point detector. However, not all expressions for *B*-factors are amenable to analytical derivation, so as an approximation, they are sometimes used as a final multiplicative constant with uncollided flux. The complication associated with practical shields are that they are often multilayered (stratified or laminated), and for them only empirical "recipes" exist how to calculate the overall or composite *B*-factor, such as historically important methods of Goldstein, Blizard, Broder and Bowman-Trubey [6]. An excellent review of historical developments of various *B*-factors can we found in papers by Trubey [7] and Harima [8].

This paper investigates further development of our one-dimensional PK program [9][10] with volumetric slab gamma source shielded by slab shields. The slabs have finite thickness but are infinite in height and width, producing a one-dimensional gamma ray transport through materials. The specific source intensity, in units # photons/(cm^3s), can be a constant value or exponentially decreasing function of a slab thickness. The later is important for simulation of secondary gamma dose rate in shields, originating from exponentially decreasing neutron flux. Even though the program is general with user-defined number of layers, this paper focuses on water-concrete combination, related to practical shields. For this two-layer shield, an exact analytical solution can be found, so it is programmed and compared to a referent Monte Carlo (MC) solution of the SCALE6.1.3 code package [11].

2 METHODS FOR COMPOSITE B-FACTOR

The variation of *B*-factor in multi-layer shields differs from that in homogeneous media due to change in the angular and energy distribution of the gamma rays penetrating the layers and when facing material discontinuities or regional boundaries [7][8]. One can notice how memory effect is present in *B*-factor, since incident radiation depends on previously penetrated layers, and that order of layers is also significant due to photon spectrum change. The accumulated experimental evidence from gamma shielding served for a development of simple methods for treating composite shields, accurate enough for practical purposes. The pioneers of the so called "analytical age" of reactor shielding development (1950-ies and 1960-ies) were scientists that made seminal contributions and helped shaping this new-established applied discipline. Some of them also worked on problems of composite shields [6] so we briefly present their ideas next, which were coded into our PK program. The C programming language [12] was used for all work presented in this paper and is based on open-source GNU compiler [13][14]. The intuitive averaging or multiplying of individual *B*-factors over different layers is out of the question, since it would result in unnecessary thick or thin shields.

2.1 Method of Goldstein

H. Goldstein, one of the initiators for the RSICC centre establishment at ORNL, proposed the homogenization of laminated shields by calculating the weighted-effective atomic number Z_{eff} of the shield using the atomic numbers Z_{i} of individual layers with "optical" thickness expressed as multiplication of real thickness x_{i} (cm) and linear attenuation coefficient μ_{i} (cm^{-1}) as

$$Z_{eff} = \frac{\sum_{i=1}^{N} Z_i \cdot \mu_i x_i}{\sum_{i=1}^{N} \mu_i x_i}. \qquad (2\text{-}1)$$

We see how composite shield is replaced with homogenized pseudo-shield with effective number Z_{eff}. Proceeding further, the composite *B*-factor would be calculated by using the linear dependence on shield thickness, or first order approximation, as follows:

$$B(Z_{eff}, \sum_{i=1}^{N} \mu_i x_i) = \alpha(Z_{eff}, E_\gamma) \sum_{i=1}^{N} \mu_i(E_\gamma) x_i \ . \quad (2\text{-}2)$$

One should bear in mind how each layer of shielding material can be made of several chemical elements (i.e. concrete), giving in turn an average atomic number defined as

$$\bar{Z} = \frac{\sum_{k=1}^{M} Z_k \cdot \frac{w_k}{A_k}}{\sum_{k=1}^{M} \frac{w_k}{A_k}}, \quad (2\text{-}3)$$

where for the *k*-th element of the mixture we have
w_k – fraction by weight
Z_k – atomic number
A_k – atomic weight

The expression for *B*-factor given is fitted over range of μx, for the various elements available in standard *B*-factor data tables using the method of least squares; this is performed for various Z-values for user defined gamma energy. The fitted values of $\alpha(Z_{eff}, E_\gamma)$ related to exposure (or dose) buildup data of Goldstein-Wilkins can be found in tables for elements H_2O, Al, Fe, Sn, W, Pb and U, spanning gamma ray energy range [0.5 - 10] MeV [6].

2.2 Method of Blizard

This method uses the last layer of shielding material as representative of the effective atomic number of the composite shield. This comes from the suggestion of E. Blizard who stated how gamma rays tend to "forget" the nature of the preceding materials, so effectively only the last layer is determinantal for emerging gamma rays. However, there is a practical limitation to this method: the last layer should not be below 3 mpfs (mean free paths) in thickness. The same procedure of Goldstein can thus be applied, using Z_{last} instead off Z_{eff}:

$$B(Z_{last}, \sum_{i=1}^{N} \mu_i x_i) = \alpha(Z_{last}, E_\gamma) \sum_{i=1}^{N} \mu_i(E_\gamma) x_i \ . \quad (2\text{-}4)$$

Our PK program will warn the user if this "at least 3 mfps" margin is broken, so the results should be taken with proper care.

2.3 Method of Broder

A more refined approach comes from Broder and other Soviet atomic energy scientists from 1960-ies, where attempt is made to allow for the passage of photons through the previous layer, by assuming the buildup contribution of each layer is additive. The total *B*-factor can be found using a method of differentiation between *N*-layers as follows:

$$B(\sum_{i=1}^{N} \mu_i x_i) = \sum_{n=1}^{N} B_n(\sum_{i=1}^{n} \mu_i x_i) - \sum_{n=2}^{N} B_n(\sum_{i=1}^{n-1} \mu_i x_i) \, . \quad (2\text{-}5)$$

A special case of only two layers is reducing Broder expression to Blizard form, i.e.,

$$B(\sum_{i=1}^{2}\mu_i x_i) = B_1(\mu_1 x_1) + B_2(\mu_1 x_1 + \mu_2 x_2) - B_2(\mu_1 x_1)\,, \tag{2-6}$$

with one additional (correction) term depending on differences in *B*-factors.

2.4 Method of Bowman-Trubey

The ORNL scientists L. Bowman and D. Trubey proposed this formula in 1960-ies for energy absorption (i.e. heating) in a 2-layer slab shield and proved to be adequate in comparison with their MC calculations. The exponential terms are related to flux saturation process in shield layers:

$$B(\sum_{i=1}^{2}\mu_i x_i) = B_1(\mu_1 x_1)B_2(\mu_2 x_2)e^{-\mu_2 x_2} + B_2(\mu_1 x_1 + \mu_2 x_2)(1 - e^{-\mu_2 x_2})\,. \tag{2-7}$$

This expression is quite useful, since it holds for any combination of two shielding materials.

3 SOURCE SLAB SHIELDED BY A SLAB SHIELD

3.1 Constant volume source

This section will present analytic derivation of the point detector flux at P following elements depicted on Figure 1. An infinite source slab has thickness *t* (cm) and is shielded with infinite slab shield of thickness *b* (cm). The linear attenuation coefficients of the source and shield materials are μ_1 and μ_2, respectively. The source slab has a constant volume emission rate of S_V (phot/cm^3/s) and is uniformly filled with material with self-absorption. The point detector P is located on the outer surface of the slab shield, for which PK method is used for deriving the gamma flux.

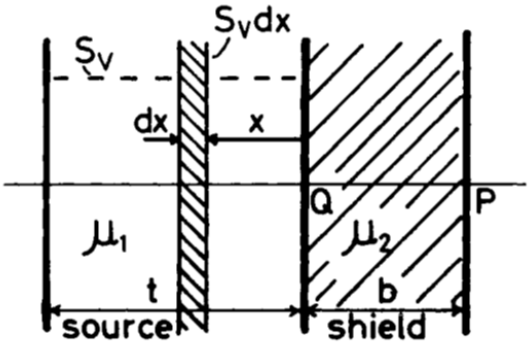

Figure 1: Geometry arrangement for the constant volume source S_V (phot/cm^3/s) shielded with a uniform slab shield [6]

The volume source can be interpreted as the sum of differential slabs of thickness *dx* (cm) which correspond to infinite planar sources of specific intensity $S_V dx$ (phot/cm^2/s). The auxiliary problem of gamma plane shielded with a slab shield of finite thickness was presented in paper [9], and uncollided gamma flux solution is in the form $(S_V dx/2)E_1(\mu_2 b)$, where exponential integral function of order $n = 1$ is a special case of a more general definition (for $x > 0$)

$$E_n(x) = x^{n-1}\int_x^\infty \frac{e^{-t}}{t^n}dt = \int_1^\infty \frac{e^{-xt}}{t^n}dt\,, \tag{3-1}$$

which can be found in various shielding handbooks [1][4]. Returning to our original problem, the PK formulation of differential gamma flux on detector P originating from planar source with thickness *dx* at distance *x* from the origin gives the following equation:

$$d\phi = \left(\frac{S_V dx}{2} \right) E_1(\mu_1 x + \mu_2 b) . \tag{3-2}$$

The uncollided gamma flux is obtained by integrating over complete source slab as

$$\phi = \frac{S_V}{2} \int_0^t E_1(\mu_1 x + \mu_2 b) dx , \tag{3-3}$$

giving in turn double integral by definition of E_1 function

$$\phi = \frac{S_V}{2} \int_0^t dx \int_1^\infty \frac{e^{-(\mu_1 x + \mu_2 b) y}}{y} dy . \tag{3-4}$$

After rearranging the order of integrands, the integration will introduce the E_2 function as

$$\phi = \frac{S_V}{2\mu_1} \left[E_2(\mu_2 b) - E_2(\mu_1 t + \mu_2 b) \right] . \tag{3-5}$$

A special case of this result, important for practical shielding application, is a thick source slab, i.e. if optical thickness $\mu_1 t$ is more than 3 mpfs, then a simplified result of sufficient accuracy becomes

$$\phi = \frac{S_V}{2\mu_1} E_2(\mu_2 b) . \tag{3-6}$$

The final step is calculation of the total buildup flux based on uncollided flux part – it was not possible to implement "classic" *B*-factors like Taylor or Berger in analytic integration since this composite shield is made from two different layers. However, approximation to buildup flux is still possible by calculating the composite *B*-factor and multiplying it with uncollided flux part. This approach was implemented in our PK program.

3.2 Exponentially decreasing volume source

This case has a great importance for practical shields, since it essentially describes secondary gamma emission, resulting from exponentially decreasing neutron flux penetrating the first layer of the shield. The neutron interactions through radiative capture will produce secondary photons which form a spatially dependent gamma source. The infinite plane slab of thickness t_1 is containing a spatially dependent volume source $S(x) = S_V e^{-\lambda x}$, where S_V (phot/cm^3/s) is constant, λ (cm^{-1}) is the source attenuation parameter and x (cm) is the source thickness variable (see Figure 2).

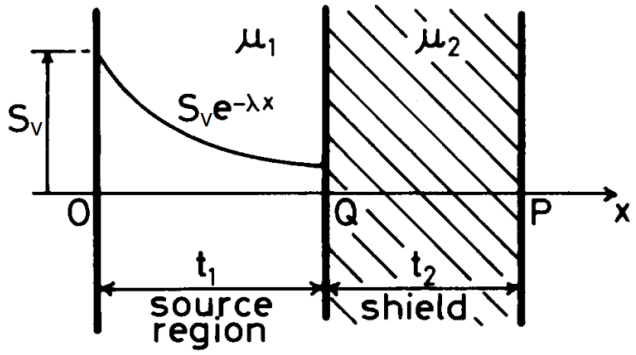

Figure 2: Geometry arrangement of the exponentially decreasing volume source $S(x) = S_V e^{-\lambda x}$ (phot/cm^3/s) shielded with a uniform slab shield [6]

The use of a simple expression for B-factor can considerably simplify the total flux derivation, and this approach was used by Wood: the B-factor of booth region has a linear form $B(\mu x) = \alpha\mu x$, where α is a known constant and assumed the same for both layers. To derive an expression for the total flux at point detector P, one must first consider an auxiliary problem of the gamma disc with radius R(cm), emitting photons isotropically with specific intensity of S_A (phot/cm^2/s), shielded by a slab shield t_2 (cm). The point detector P is on the outer surface of the shield at the position a (cm) from the origin, giving the boundary angle of $\theta = arctg(R/a)$. Figure 3 gives the geometry setup.

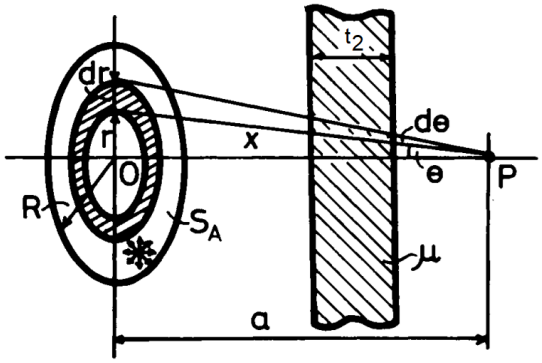

Figure 3: Geometry arrangement for the isotropic gamma disc shielded with a slab shield [6]

Using the PK approach with analytical integration, one obtains the total flux at P as

$$\phi_d = \frac{S_A}{2}\alpha\left[e^{-\mu t_2} - e^{-\mu t_2 \sec\theta}\right], \tag{3-7}$$

which can easily be transformed into a plane solution by letting $\theta \to \pi/2$ and $R \to \infty$:

$$\phi_p = \frac{S_A}{2}\alpha e^{-\mu t_2}, \tag{3-8}$$

where $\mu_2 t_2$ is the optical thickness of the shield in mfps.

Using this auxiliary solution, one can return to the original problem and notice in Figure 4. how the volume source consists of infinite plane elements of thickness dx, with specific intensity $S_A = S(x)dx$ (phot/cm^3/s), for which the flux solution is already known.

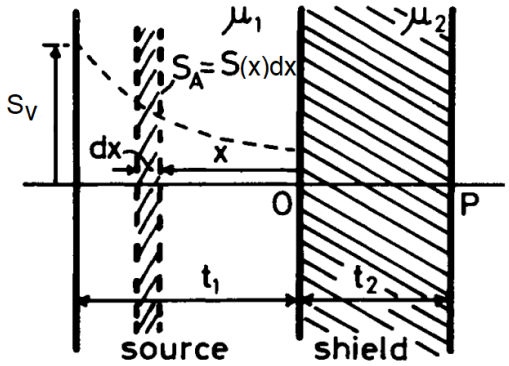

Figure 4: Geometry arrangement of the exponentially decreasing volume source with s slab shield and new position of the origin x=0 [6]

By adjusting the origin x = 0 between the two layers, one can proceed with usual PK definition for the differential gamma flux at position P due to the plane element dx at x:

$$d\phi = \frac{S(x)dx}{2}\alpha e^{-(\mu_1 x+\mu_2 t_2)}, \tag{3-9}$$

where exponentially decreasing source now has transformed spatial variable as $S(x) = S_V e^{-\lambda(t_1-x)}$. The integral to be solved is elementary one:

$$\phi = \frac{S_V}{2}\alpha e^{-(\lambda t_1+\mu_2 t_2)}\int_0^{t_1} e^{-(\mu_1-\lambda)x}dx\,. \tag{3-10}$$

The total gamma flux at P due to exponentially decreasing source becomes

$$\phi = \frac{S_V}{2}\alpha\frac{e^{-\mu_2 t_2}}{\mu_1-\lambda}\left[e^{-\lambda t_1}-e^{-\mu_1 t_1}\right]. \tag{3-11}$$

The specific form of the solution will depend on the relationship between μ_1 and λ, i.e. which attenuating factor is a more dominant one. This solution provided by Wood is based on the first order *B*-factor (i.e. linear function), which significantly simplifies analytical derivation of the total flux. This procedure, however, introduces an underestimation in total flux, as will be shown later. Different approaches to this problem are possible, and author's method is presented next for an uncollided flux derivation, which should be folded with the composite *B*-factor. Using Figure 2 as a starting point, and setting x=0 at the left boundary, the PK differential flux at P is

$$\phi_u = \frac{S_V}{2}\int_0^{t_1} e^{-\lambda x}E_1(\mu_1 x+\mu_2 t_2)dx\,. \tag{3-12}$$

Using the substitution of $y = \mu_1 x + \mu_2 t_2$ one transforms this integral into a form

$$\phi_u = \frac{S_V}{2\mu_1}e^{(\lambda/\mu_1)\mu_2 t_2}\int_{y=\mu_2 t_2}^{\mu_1 t_1+\mu_2 t_2} e^{-(\lambda/\mu_1)y}E_1(y)dy\,, \tag{3-13}$$

and by using the general property of E_1 function

$$I = \int e^{zy}E_1(y)dy = \frac{1}{z}\left[e^{zy}E_1(y)-E_1(y(1-z))\right], \tag{3-14}$$

one can evaluate the integral I for our specific case as:

$$I = -\frac{\mu_1}{\lambda}\left[\begin{array}{l} e^{-(\lambda/\mu_1)\mu_2 t_2}\left\{e^{-\lambda t_1}E_1(\mu_1 t_1+\mu_2 t_2)-E_1(\mu_2 t_2)\right\}- \\ E_1\left((\mu_1 t_1+\mu_2 t_2)(1+\frac{\lambda}{\mu_1})\right)+E_1\left(\mu_2 t_2(1+\frac{\lambda}{\mu_1})\right)\end{array}\right]. \tag{3-15}$$

Inserting the obtained integral I into the uncollided flux solution, one finally obtains

$$\phi_u = \frac{S_V}{2\lambda}\left[\begin{array}{l} E_1(\mu_2 t_2)-e^{-\lambda t_1}E_1(\mu_1 t_1+\mu_2 t_2)- \\ e^{(\lambda/\mu_1)\mu_2 t_2}\left\{E_1\left(\mu_2 t_2(1+\frac{\lambda}{\mu_1})\right)-E_1\left((\mu_1 t_1+\mu_2 t_2)(1+\frac{\lambda}{\mu_1})\right)\right\}\end{array}\right]. \tag{3-16}$$

One should notice the following properties of the flux in Eq. (3-16):

- first part is due to finite thickness of the source slab
- second part is correction due to distributed source
- expression is general and has always positive arguments of E_1 function

From the programming perspective, this solution is straightforward to implement since no comparison between λ and μ_1 is needed in determining $E_1(x)$ value, which is defined only for $x>0$. Chilton [5] also provided variant of general solution to uncollided flux, but it is conditional in the following way (when $t_2 \neq 0$):

a) case $\lambda \neq \mu_1$

$$\phi_u = \frac{S_V}{2\lambda}\left[\begin{array}{l} e^{\lambda t_1}E_1(\mu_1 t_1+\mu_2 t_2)-E_1(\mu_2 t_2)- \\ e^{-(\lambda/\mu_1)\mu_2 t_2}E_1\left((\mu_1 t_1+\mu_2 t_2)(\frac{\mu_1-\lambda}{\mu_1})\right)+e^{-(\lambda/\mu_1)\mu_2 t_2}E_1\left(\mu_2 t_2(\frac{\mu_1-\lambda}{\mu_1})\right) \end{array}\right] \quad (3\text{-}17)$$

b) case $\lambda = \mu_1$

$$\phi_u = \frac{S_V}{2\mu_1}\left[e^{\mu_1 t_1}E_1(\mu_1 t_1+\mu_2 t_2)-E_1(\mu_2 t_2)+e^{-\mu_2 t_2}\ln\left(1+\frac{\mu_1 t_1}{\mu_2 t_2}\right)\right] \quad (3\text{-}18)$$

In both Chilton cases the source attenuation parameter λ can have an arbitrary sign, effectively modelling slab source with exponential increase or decrease, so cases of negative $E_1(x)$ argument can occur. This is handled by introduction of general exponential integral $E_i(x)$ with analytical continuation property, to circumvent the E_1 singularity at $x = 0$:

$$E_i(x) = -\int_{-x}^{\infty}\frac{e^{-t}}{t}dt = \int_{-\infty}^{x}\frac{e^{-t}}{t}dt \text{ , for } x > 0. \quad (3\text{-}19)$$

For positive value of x, it is equivalent to $E_1(x)$, and for negative x it is $E_1(-x) = -E_i(x)$.

The special case when the second material layer is not present ($t_2 \to 0$) gives the solution

$$\phi_u = \frac{S_V}{2\lambda}\left[e^{\lambda t_1}E_1(\mu_1 t_1)-E_1\left(\mu_1 t_1(\frac{\mu_1-\lambda}{\mu_1})\right)-\ln\left(\frac{\mu_1-\lambda}{\mu_1}\right)\right]. \quad (3\text{-}20)$$

One can notice how Chilton approach demands more programming effort, and for efficient coding one should consult numerical methods by Press et al [15]. The PK program implements all three types of the flux solution presented (Wood, authors, Chilton) and composite *B*-factors (Goldstein, Blizard, Broder, Bowman-Trubey) for obtaining the buildup flux. The comparison of PK results with MAVRIC shielding sequence of SCALE6.1.3 code is presented next for the purpose of data verification.

4 COMPARISON OF PK AND MC RESULTS

4.1 Constant volume source

The test case was isotropic volume source of water (25 cm) emitting 1 MeV gamma rays with total intensity of 1.0 phot/s, shielded by an ordinary concrete layer (25 cm). The height and width of slabs were 200 cm which resulted in specific source intensity of $1.0\cdot10^{-6}$ phot/cm^3/s in water. The gamma flux was calculated on the slab shield external surface using the hybrid CADIS methodology of MAVRIC [11]. The results for gamma group 12 (1.0-0.8 MeV), capturing the source emission energy, show distribution of photons through shield layers with their relative MC errors (Figure 5). The uncollided MC flux at the detector was $3.39\cdot10^{-8}$ phot/cm^2/s ± 0.04%, while the total flux was $5.51\cdot10^{-7}$ phot/cm^2/s ± 0.9%.

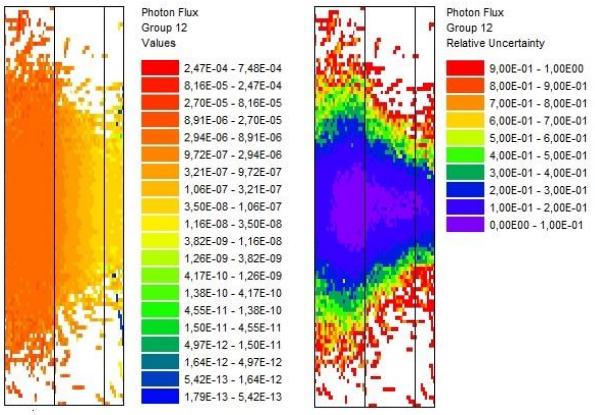

Figure 5: MAVRIC gamma flux solution with relative errors (photon group 12)

The composite *B*-factors of water-concrete shield was 15.9, 14.2 and 10.0 for Goldstein, Blizard and Broder, respectively. Taking the first one as the most conservative, one obtains buildup flux of $4.32 \cdot 10^{-7}$ phot/cm^2/s, while uncollided flux part was $2.72 \cdot 10^{-8}$ phot/cm^2/s. This PK-to-MC flux difference is only -22%, but CPU time for PK (< 1 ms) is only a fraction of MC time (12 min), giving significant speedup for a little loss of accuracy. This agreement will deteriorate when increasing the concrete thickness from 25 cm to 100 cm (25 cm step). Figure 6 shows the comparison of total fluxes on outer shield surface, while PK-to-MC relative errors are shown in Figure 7 for uncollided and total flux components.

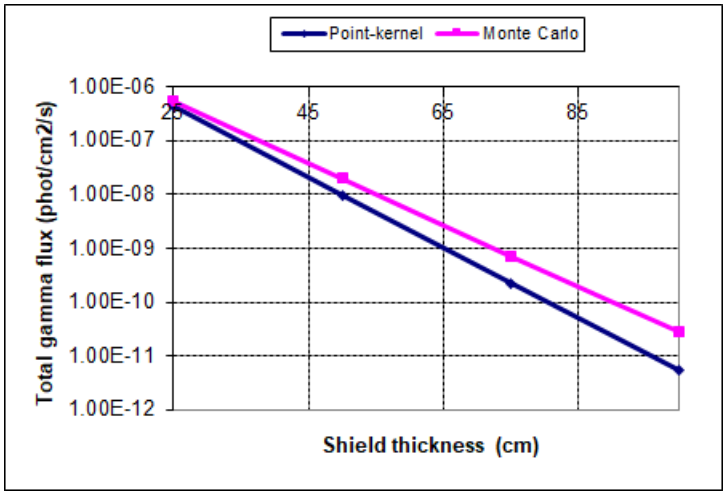

Figure 6: Total PK and MC gamma flux for 1 MeV gamma rays in concrete

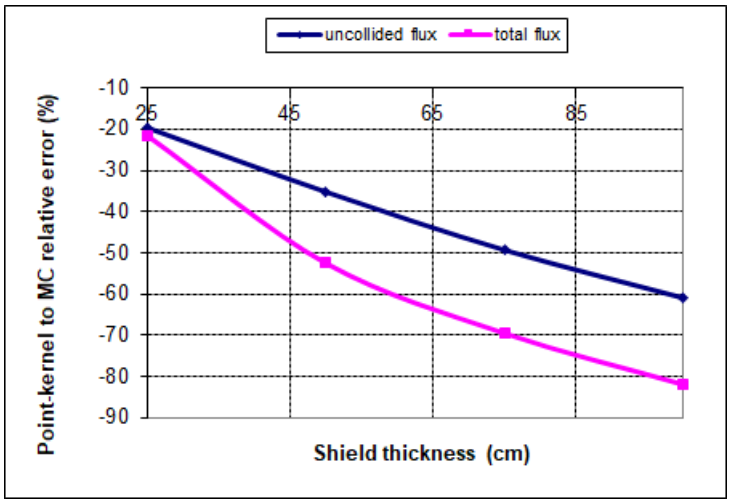

Figure 7: PK-to-MC relative error for 1 MeV gamma rays in concrete

This flux difference is significant only in a relative sense, but not in an absolute way, since the transmitted gamma flux is very small with order of $1.0 \cdot 10^{-13}$. It is also interesting to compare different composite *B*-factor profiles with increasing thickness of the concrete layer. The Goldstein model of shield homogenization proved to be most conservative one, so it was implemented as a default option in the PK program for total flux calculation. One should notice how these composite *B*-factor models converge to the same limiting value for a very thick shield.

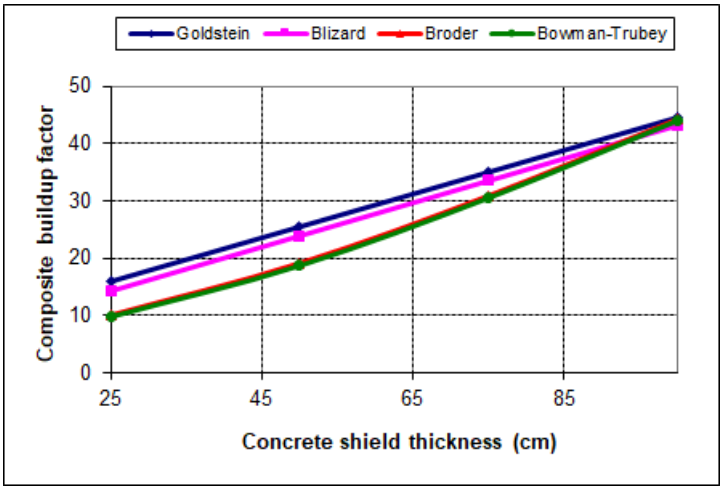

Figure 8: Comparison of different composite *B*-factor models

4.2 Exponential volume source

This section gives sensitivity study of the source attenuation coefficient λ, i.e. its influence on the point detector gamma flux and relation to linear attenuation coefficient μ_1 of the water. As already mentioned, this case renders a practical problem where exponentially decreasing neutron flux in a slab gives rise to a source of secondary photons. This case differs from the shielding problem of constant volumetric gamma source, often present in uniform mixtures of radioactive material, such as waste.

The test case to be considered is again water-concrete composite shield, each layer 25 cm thick, but with much larger height and width (10 m). The source photons of 1 MeV are uniformly sampled in the water layer with decreasing distribution in *x*-axis, ranging from 0 to 10 in the λ-parameter. This will relate different values of λ with μ_1 and promote conditional PK solution to exiting gamma flux. It means that, on one hand, the concrete can produce higher attenuation ($\lambda < \mu_1$) compared to source weakening in water, meaning point detector will be dominated by closer source regions. On other hand, the source can be concentrated at the very beginning ($\lambda > \mu_1$), meaning detector domination with farthest source regions. The unlikely "resonant" case ($\lambda = \mu_1$) will occur when the exponential source attenuation in water equals photon attenuation in the concrete layer.

The MAVRIC photon flux detail in central part of the slabs is shown in Figure 9, together with relative errors for two extreme values of λ-parameter. Comparison is bringing together weak vs. strong source exponential distribution, relative to the linear attenuation coefficient of water (~ 0.07 cm^{-1}). The Figure 9 also confirms aforementioned theoretical findings through MC sampling, i.e. on the right we see discrimination of low-contributing photons in water closer to concrete.

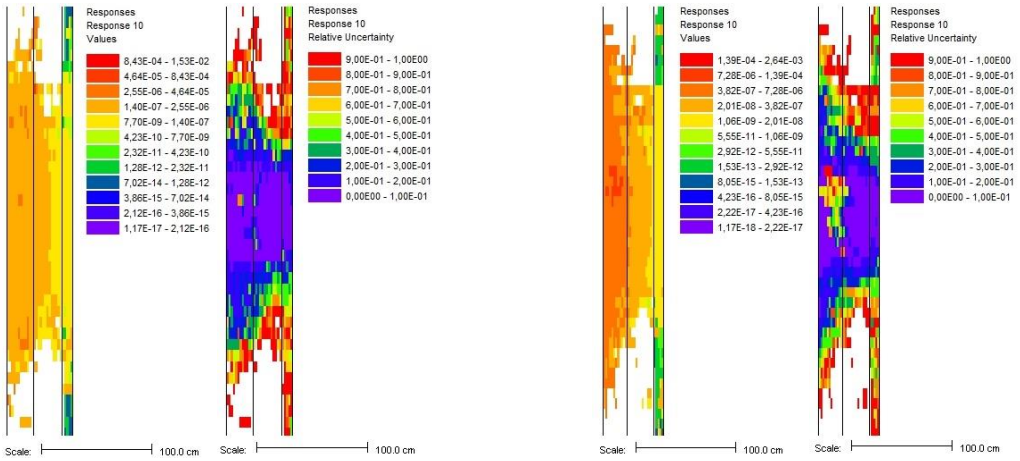

Figure 9: MAVRIC gamma flux distribution for λ=0.001 (left) and λ=10 (right)

Chilton and authors solution resulted in practically the same PK results for uncollided and total gamma flux, and they are more conservative relative to Wood approach. The comparison of PK solutions to MAVRIC MC solution is shown in Figure 10. The specific photon source in water was $S_V = 4.0 \cdot 10^{-8}$ phot/cm^3/s and linear attenuation coefficient of layers was 0.0706 cm^{-1} for water and 0.1492 cm^{-1} for concrete, respectively. The MC was used with $1.0 \cdot 10^6$ photon histories with an average CPU time of 6 min per different λ-case, giving in turn point detector flux relative error of 0.1% on average. It was interesting to notice how *B*-factor for MC solution increased steadily from 16 to 21 when λ-parameter increased from 0 to 10. For PK flux solution the composite *B*-factor of Goldstein was highest with 15.9 (Blizard 14.2, Broder 10, Bowman-Trubey 9.9).

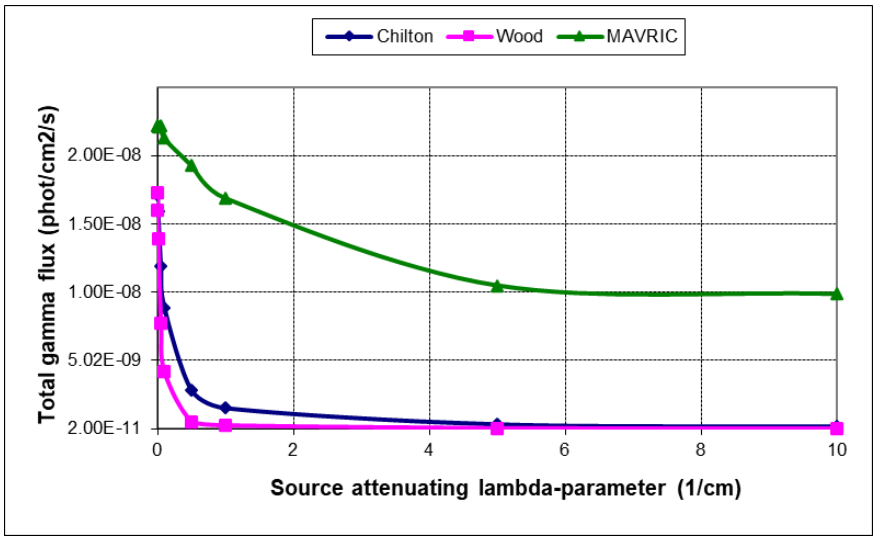

Figure 10: Comparison of PK (Chilton and Wood) and MC total flux solution for a range of λ-parameter values (from 0 to 10) in $S(x) = S_V e^{-\lambda x}$

The obtained PK(Chilton)-to-MC relative errors of total gamma flux proved to be rather sensitive to numerical difference between λ-parameter of the source and linear attenuation coefficient of the source (μ_1 = 0.07 cm^{-1}). Figure 11 shows relative error ranging from -22% to -98% for λ-values in range 0 to 10. One should also note that λ = 0 reduces to the case of constant volume source. This difference PK vs. MC should be attributed to explicit 3D scattering photon physics module inside MC simulation, not traceable with PK approximative method, since photon energy is kept constant for all computational data and routines. This "constant energy" demonstrates one of the limitations in the PK method, but it is compensated with a high CPU time speedup relative to MC simulation.

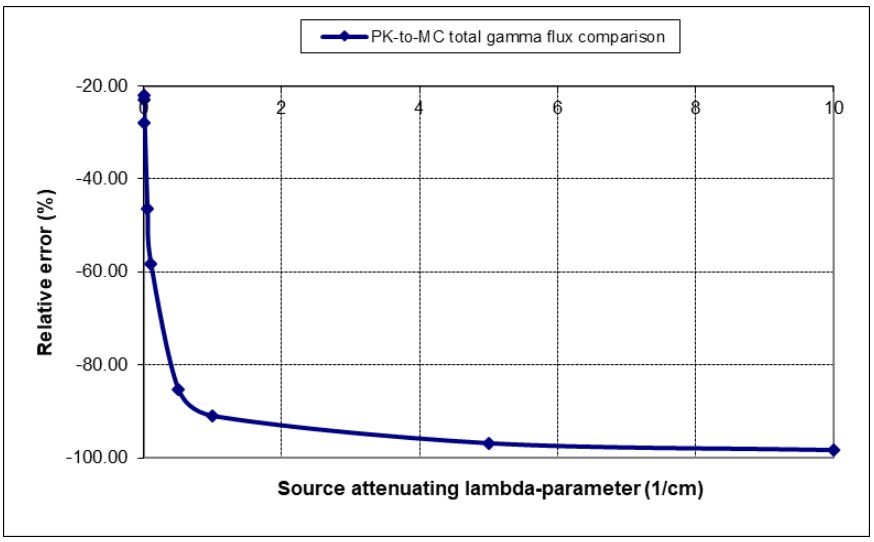

Figure 11: Relative error of PK (Chilton) to MC total flux solution for a range of λ-parameter values (from 0 to 10)

5 CONCLUSION

The development of the PK program for basic gamma radiation shielding is still an ongoing project, encompassing various source shapes shielded with basic slab shields. This paper presents further development of the program with volumetric gamma sources which now have the option of exponential spatial distribution opposed to a constant one. In conjunction to programming analytical flux solutions for a two-slab shield geometry (Chilton and Wood), the methods of composite *B*-factor calculation were also included. In this way, the PK program user has an ability to define the thickness of the two slabs, material compositions, energy of gamma rays, specific source intensity, and to proceed with calculation of layer-based *B*-factors (Taylor or Berger), overall composite *B*-factor, uncollided and total gamma flux and finally flux-to-dose rate response. The verification of PK results for selected test cases has been carried out using MAVRIC shielding sequence of SCALE6.1.3 code package. A generally good agreement of 1D PK solution to explicit 3D MC result was obtained for selection of "reasonable" concrete thickness and source λ-parameter, rendering similar systematic trends in gamma flux curve profiles. The PK-to-MC underprediction in gamma fluxes is due to inherent PK method inability to properly include gamma scattering, so corrective *B*-factor concept is much needed as a valuable substitution for radiation streaming and backscattering with angle-dependent peaks.

ACKNOWLEDGMENTS

This work was supported by the Croatian Science Foundation under the project number HRZZ-IP-2024-05-4011.

REFERENCES

[1] T. Rockwel III (Ed.), Reactor Shielding Design Manual, USAEC Report TID-7004, 1956.

[2] H. Goldstein, Fundamental Aspects of Reactor Shielding, Reading, Mass., Addison-Wesley Publishing Company, 1959.

[3] S. Glasstone, A. Sesonske, Nuclear Reactor Engineering - Reactor Design Basics, 4th edition Volume One, Chapman & Hall, New York, 1994.

[4] N.M. Schaeffer, Reactor Shielding for Nuclear Engineers, U.S. Atomic Energy Commission, Office of Information Services, 1973.

[5] A.B. Chilton, J.K. Shultis, R.E. Faw, Principles of Radiation Shielding, Prentice-Hall, Inc., Englewood Cliffs, New Jersey, 1984.

[6] J. Wood, Computational Methods in Reactor Shielding, Pergamon Press, Oxford, UK, 1982.

[7] D.K. Trubey, History and Evolution of Buildup Factors, *In Proceedings of a Special Session for the Radiation Protection and Shielding Division at the American Nuclear Society Winter Meeting*, ORNL/RSIC-55 Early Test Facilities and Analytic Methods for Radiation Shielding, Chicago, IL, USA, 15–20 November 1992, pp. 47-53.

[8] Y. Harima, An Historical Review and Current Status of Buildup Factor Calculations and Applications, *Radiation Physics and Chemistry*, Vol. 41, pp. 631–672, 1993.

[9] M. Matijević, K. Trontl, S. Šadek, P. Družijanić, Point-Kernel Code Development for Gamma-Ray Shielding Applications, *Applied Sciences*, 15, 7795, pp. 1–25, 2025.

[10] M. Matijević, A. Kaselj, K. Trontl, Point-Kernel Shielding Applications of Sievert Integral, *Journal of Energy – Energija*, Vol. 74, No. 4, pp. 22-29, 2025.

[11] "SCALE: A Comprehensive Modeling and Simulation Suite for Nuclear Safety Analysis and Design", ORNL/TM-2005/39, Version 6.1, June 2011. Available from Radiation Safety Information Computational Center at Oak Ridge National Laboratory as CCC-785.

[12] B.W. Kernighan, D.M. Ritchie, The C Programming Language, 2nd edition, Prentice Hall PTR: Saddle River, NJ, USA, 1988.

[13] The GNU C Compiler. Available online: https://gcc.gnu.org/ (accessed on 26 March 2026).

[14] The GNU C Language Intro and Reference Manual. Available online: https://www.gnu.org/software/c-intro-and-ref/manual/ (accessed on 26 March 2026).

[15] W.H. Press, S.A. Teukolsky, W.T. Vetterling, B.P. Flannery, Numerical Recipes in C - The Art of Scientific Computing, 2nd ed., Cambridge University Press, New York, USA, pp. 222–225, 1992.